Applied Catalysis B: Environmental 163 (2015) 623–627

Contents lists available at ScienceDirect

Applied Catalysis B: Environmental

journal homepage: www.elsevier.com/locate/apcatb

Metal oxides/CNT nano-composite catalysts for oxygen reduction/oxygen evolution in alkaline media

Nalin I. Andersen [1], Alexey Serov [1], Plamen Atanassov *

Department of Chemical and Nuclear Engineering, 1 University of New Mexico, University of New Mexico, Albuquerque, NM 87131, USA

ARTICLE INFO

Article history:
Received 8 April 2014
Received in revised form 17 July 2014
Accepted 20 August 2014
Available online 27 August 2014

Keywords:
Oxygen reduction catalyst
Oxygen evolution catalyst
Non-platinum group catalyst
Environmental catalysts
Functionalized carbon nanotubes

ABSTRACT

A series of highly active state-of-the-art catalysts have been synthesized by depositing high loadings of transition metal oxides (MnO_2, Co_3O_4, NiO, CuO and Fe_xO_y) onto nitrogen-doped carbon nanotubes (CNTs) for bi-functional catalysis in alkaline media. The metal oxides have been dispersed onto functionalized CNTs by an improved impregnation method. This novel, synthetic approach allows for both the preparation of functionalized nitrogen-doped CNTs as well as the even dispersion of metal oxides onto the walls of the CNTs. The catalysts have been characterized by Brunauer–Emmett–Teller (BET), scanning electron microscopy (SEM), transition electron microscopy (TEM), X-ray diffraction (XRD) and X-ray photoelectron spectroscopy (XPS) methods. Catalytic activity has been measured using a Rotating Disc Electrode (RDE) experiment. The resulting catalysts are stable in alkaline media under experimental conditions and have high bi-functional electrocatalytic activity—both for the oxygen reduction reactions (ORR) and oxygen evolution reactions (OER). From this series of catalysts, the most active catalyst for ORR is the 50 wt% MnO_2/CNT catalyst with a half-wave potential of 0.84 V at the current density of $-2.1\ mA\ cm^{-2}$ and an onset at 0.98 V versus RHE. The most active for OER is the 50 wt% NiO/CNT catalyst with an onset potential at 1.45 V versus RHE.

1. Introduction

The majority of our world's vehicles are dependent on petroleum-derived fuels. The craving for these fuels has led to political unrest, wars, poverty and mass pollution. Furthermore, the conversion efficiency of chemical potential energy into kinetic energy from these fuels is quite low for an internal combustion engine. Fuel cell technology has been extensively researched to address these issues. Fundamentally, these fuel cells are driven by electrochemical kinetics and intrinsic kinetics at the catalyst layer. Recently, interest to catalysts that can reduce oxygen during the cathodic cycles and evolve oxygen during anodic cycles (bi-functional catalysts) has significantly grown from manufacturers of metal-air batteries, electrolyzers and fuel cells. Presently, the most conventional cathodic and anodic catalysts are made from Pt-group metals (PGM). It has also been discovered that by placing these on commercial carbon supports that have high surface area, it enhances their activity [1]. The main drawback and need for more catalyst research is the incredibly high cost and low abundance of Pt-group elements. In recognition of the unfavorable factors that PGM-based materials possess, composite nanomaterials incorporating transition metal nanoparticles on multiwalled carbon nanotubes (MWCNTs) is described in this manuscript that rival the electrochemical activities of published PGM results.

We show through our analysis that this family of catalysts is stable in alkaline media, have large surface area, is easy to synthesize, can be produced at lower cost from abundant transition metals and still have high bi-functional electrocatalytic activity. Reported here is a method of functionalized CNT preparation based on the sacrificial support method (SSM) developed at UNM [2–14], synthesis, characterization, and electrocatalytic activity of 50 wt% MO_x/CNT hybrid catalysts in ORR and OER. The method of CNT synthesis allows for controllable production and high deposition of metal oxides. It has been reported that the preparation of composite materials based on transition metal oxides and carbon supports can be synthesized by a variety of methods; however, such high transition metal oxide loadings have not been reported in literature with bi-functional capabilities. Electrocatalysts have been synthesized by coating commercial CNTs with small loadings of transition metal oxides [15–17] and a bi-functional catalyst has been made by separately synthesizing MnO_2 nanotube structures and CNTs, followed by physically mixing the two together to create a heterogeneous

* Corresponding author. Tel.: +1 505 277 2640; fax: +1 505 277 5433.
E-mail address: plamen@unm.edu (P. Atanassov).
[1] Both authors contributed equally.

http://dx.doi.org/10.1016/j.apcatb.2014.08.033
0926-3373/

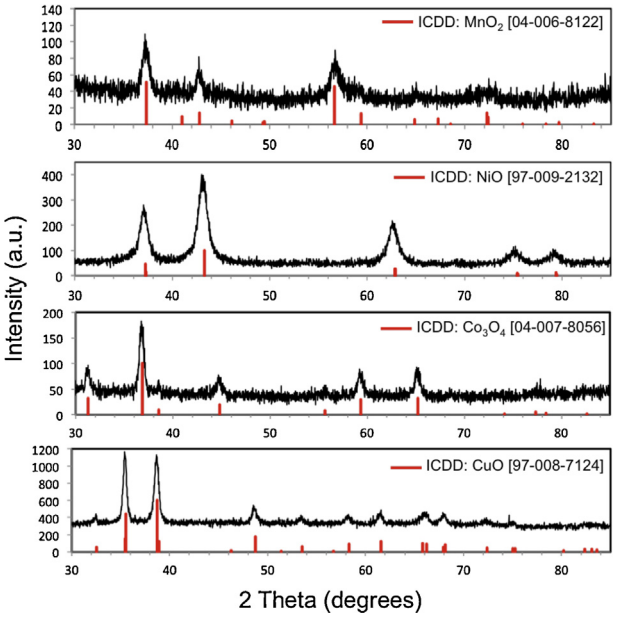

Fig. 1. XRD data for (a) 50 wt% MnO_2/CNT, (b) 50 wt% NiO/CNT, (c) 50 wt% Co_3O_4/CNT and (d) 50 wt% CuO/CNT.

mixture of compounds [18], rather than a singular nanocomposite structural network as described in the present work. The Shao-Horn group has reported state-of-the-art perovskite catalysts based on La, Cu, Mn, Co and Ni mixed oxides supported on Vulcan carbon with $E_{1/2}$ = 0.64–0.71 V [19]. The 50 wt% MnO_2/CNT catalyst presented in this research has a half-wave potential ~100 mV better than these results. The electrochemical activity is a result of the novel synthetic approach to yield specialized bi-functional nanocomposite materials, which reiterates the understanding that the method of preparing oxides and their composites affects their morphology and electrocatalytic activities.

2. Materials and methods

2.1. Catalyst synthesis

The CNTs were synthesized by a conversion of C_2H_4 on Fe nanoparticles using the sacrificial support method. $Fe(NO_3)_3$ was mixed with a colloidal suspension of a silica sacrificial support (Cab-O-Sil® EH-5, 380 $m^2\ g^{-1}$), dried and ball milled for 4 h at 450 RPM (Across International PQ-N04 Planetary Ball Mill) and placed in a furnace. The powder sample was exposed to a heat treatment at 500 °C in a H_2 atmosphere for 30 min, 760 °C in a C_2H_4 atmosphere for 60 min and 900 °C under an NH_3 atmosphere for 60 min. The results from the XPS analysis confirms the presence of nitrogen defects on the surface of the nanotubes from the introduction of ammonia, which in turn, acts as anchors for the oxides. All gases used were ultra high-grade purity. The material was removed from the furnace, leached with HF and washed to reach a neutral pH. Concentrated nitric acid is introduced, resulting in CNTs with no amorphous carbon. An impregnation method was then utilized in which liquid transition metal nitrates (99.98%, Sigma-Aldrich) were deposited on the CNT powder to yield 50 wt% metal oxides, referred to as MO_x, deposited on the CNTs. The resulting material was dried overnight in the presence of oxygen at 85 °C leaving a metal salt catalyst. After drying, the MO_x/CNTs (M: Fe, Mn, Ni, Co, Cu) were calcined at 350 °C for 120 min. This synthesis method was chosen to keep the metal oxide agglomerations as small as possible to allow for maximum active sites per catalyst mass.

2.2. Catalyst characterization

The catalysts were characterized by Brunauer–Emmet–Teller (BET) measurements, SEM (Hitachi S-5200), TEM (JEOL 2010 EX HREM), XRD (Scintag Pad V, Cu anode) and XPS (XPS spectra were acquired on a Kratos Axis DLD Ultra X-ray photoelectron spectrometer using an Al Kα source monochromatic operating at 150 W with no charge compensation) methods. Catalytic activity for ORR and OER were measured in 1.0 M KOH, prepared from deionized water and KOH pellets (99.99%, Sigma-Aldrich) using the RDE method. The

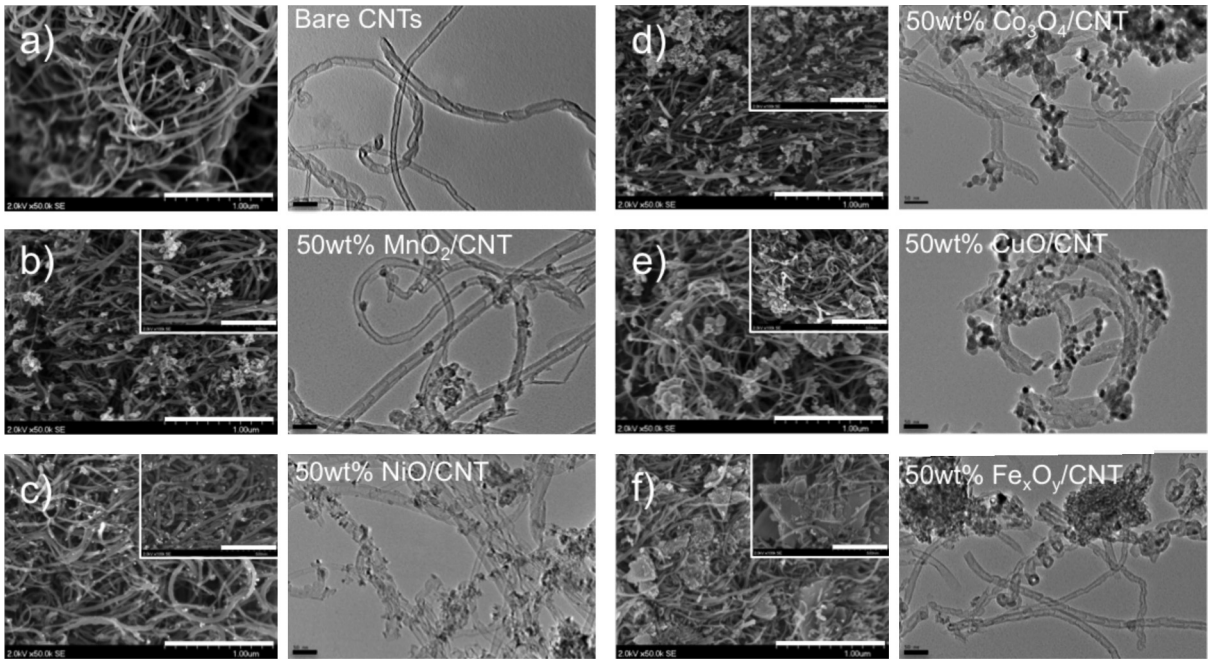

Fig. 2. SEM (left) and TEM (right) images of: (a) bare CNTs, (b) 50 wt% MnO_2/CNT, (c) 50 wt% NiO/CNT, (d) 50 wt% Co_3O_4/CNT, (e) 50 wt% CuO/CNT and (f) 50 wt% Fe_xO_y/CNT. SEM: scale bar is 1.00 μm and insets have a scale bar of 500 nm. TEM: scale bar is 50 nm.

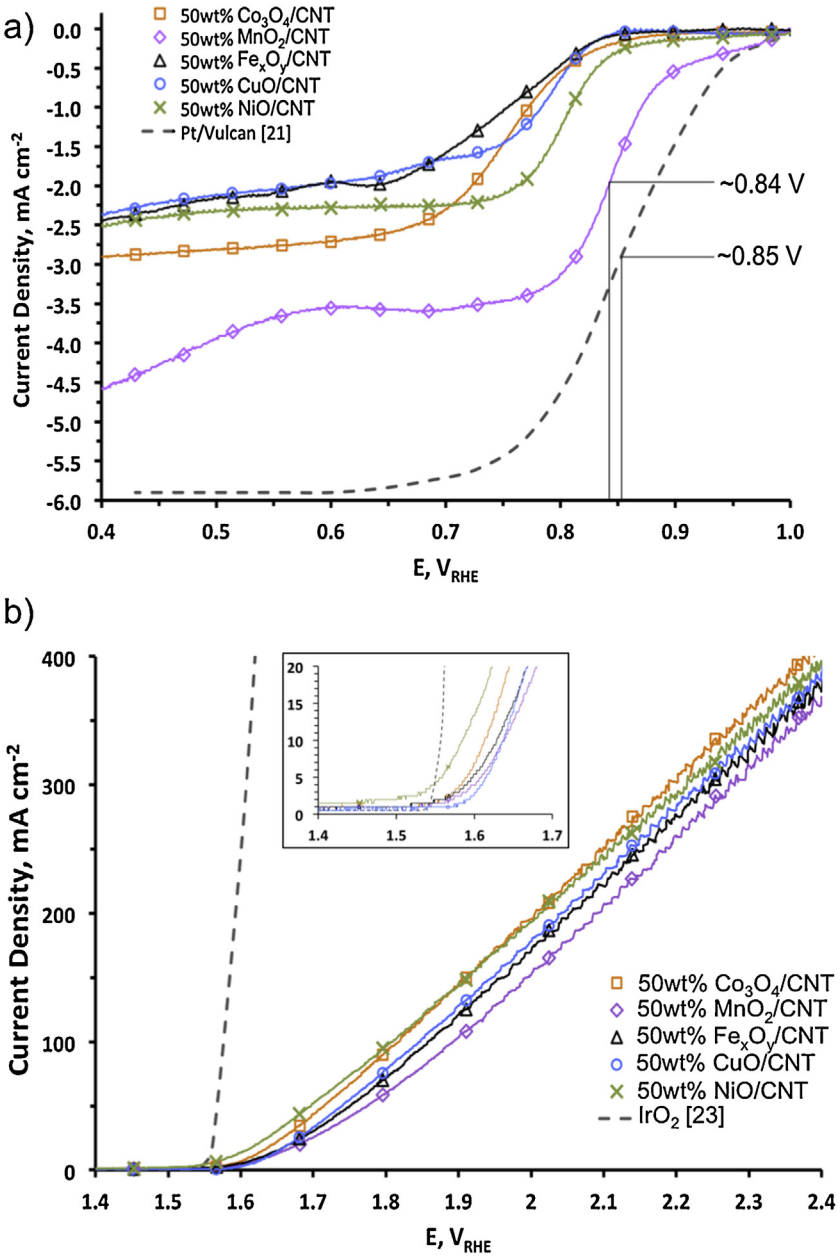

Fig. 3. Electrochemical data for 50 wt% MO_x/CNT (M: Co, Mn, Fe, Cu, Ni) catalysts, (a) ORR and (b) OER.

counter electrode used was a Pt wire and the reference electrode was a Hg/HgO reference electrode corresponding to a reversible hydrogen electrode (RHE) of 0.926 at 25 °C. The inks for the RDE experiments were prepared by mixing the catalyst powder with an optimized amount of the ionomer Nafion™ in an isopropyl alcohol/H_2O solution. The Nafion™ is used as a binder to hold the nanoparticles of the catalyst onto the electrode surface. Homogeneity of the inks was achieved by means of sonication using an ultrasound probe. Electrochemical measurements occurred with a catalyst loading of 0.2 mg cm^{-2} on a rotating disk electrode at 1600 RPM and a scan rate of 10 mV s^{-1} (Pine Instrument).

3. Results and discussion

Five composite nanomaterials consisting of deposited metal oxides (MnO_2, Co_3O_4, NiO, CuO and Fe_xO_y) onto functionalized CNTs were synthesized and characterized in this study. The 50 wt% loading of metal oxides on the CNTs was selected due to the requirement of high electric conductivity of the final catalysts. Concurrently, a smaller presence of carbon in the final material increased the durability during the OER cycles. The XRD analysis shows the formation of desirable phases (Fig. 1) confirming that the decomposition temperature of nitrates was in the range where oxides are formed and the CNTs are still stable. The functionalized CNTs were produced using the SSM method [2–14], in which an iron precursor is dispersed in a colloidal suspension of a sacrificial support, then is decomposed and reduces to form crystallite seeds. The size of these metal seeds dictates the outer diameter of the CNTs. In the present work, these seeds come from Fe(III) nitrate and the crystallite seeds were designed to be in the range of 40–60 nm in diameter. By using this method, total morphological control of the CNTs is achieved and high loadings of transition metal oxides can be coated onto the surfaces.

The morphology of the catalysts was characterized by SEM imaging (Fig. 2 (left)). The CNTs have a diameter averaging from 40 to 60 nm, indicative of the size of the Fe crystallites formed during

Table 1
BET surface areas of 50 wt% MO_x/CNT catalysts.

Catalyst	Surface area [$m^2\ g^{-1}$]
Bare CNTs	128
50 wt% Co_3O_4/CNT	60
50 wt% MnO_2/CNT	83
50 wt% Fe_xO_y/CNT	136
50 wt% CuO/CNT	72
50 wt% NiO/CNT	134

the H_2 purging phase of the synthesis, suggesting these are multi-walled carbon nanotubes. In the following descriptions, the term, "particle," will be used to describe the metal oxide deposited onto the CNTs. It was observed that the 50 wt% MnO_2/CNT catalyst has a large size distribution of oxide particles deposited onto the CNTs ranging from 8 nm to 500 nm oxide particles (Fig. 2b). Images of the 50 wt% NiO/CNT catalyst reveals evenly distributed oxide on the nanotube surfaces with little agglomeration and average particle sizes of 5 nm (Fig. 2c). The 50 wt% Co_3O_4/CNT catalyst has particle sizes from 25–200 nm with minimal agglomeration (Fig. 2d). The 50 wt% CuO/CNT catalyst has smooth oxide particles dispersed on the CNTs from 25–400 nm in size (Fig. 2e). The 50 wt% Fe_xO_y/CNT catalyst was electrochemically outperformed by all others in this series; its features include nanotubes wrapped around shattered, crystalline oxide shards up to 800 nm in size (Fig. 2f).

TEM images of the catalysts are shown in Fig. 2 in the right columns. The TEM images show that the particle size and distribution are consistent with the SEM images. From Fig. 2c, it is shown that the NiO particles are distributed evenly on the CNT surfaces. In contrast, and in reference to Fig. 2f the Fe_xO_y particles have agglomerated, leaving several hundred nanometers of CNTs bare.

The specific surface areas of the synthesized catalysts are in Table 1 and indicate the surface area per gram of catalyst synthesized. The bare CNTs have a surface area of 128 $m^2\ g^{-1}$ of CNTs synthesized. The decrease in surface area from the bare CNTs after metal deposition for the 50 wt% Co_3O_4/CNT, 50 wt% MnO_2/CNT and 50 wt% CuO/CNT may be due to the oxide particles forming inside the CNTs, since their particle sizes can be frequently less than the diameter of the CNTs. This internal tube blockage would lead to decreased surface area by BET measurements.

The electrochemical activity of the five catalysts is compared. We show through our RDE analysis in Fig. 3 that the best performers for the cathodic and anodic cycles are the 50 wt% MnO_2/CNT catalyst and the 50 wt% NiO/CNT catalyst, respectively. The poorest performer of this series is the 50 wt% Fe_xO_y/CNT catalyst. The ORR and OER of the 5 catalysts are shown in Fig. 3a and b, respectively. From the RDE results, it was determined that the 50 wt% MnO_2/CNT catalyst is the most active for ORR from its half wave potential of 0.84 V at the current density of −2 mA cm^{-2} and an onset at ~0.98 V versus RHE. This half-wave potential is within 10 mV of the reported results for carbon-supported Pt cathode catalysts reported by Gasteiger et al. [21]. as well as the polycrystalline bimetallic Pt alloys reported by Greeley et al. [22]. The 50 wt% NiO/CNT catalyst is the most active for OER with an onset potential at 1.45 V versus RHE, which is within 0.05 V of bulk Ru, which is the best performing anodic catalyst reported by Reier et al. [23].

Typically, state-of-the-art OER catalysts are unsupported materials due to the degradation of carbon during the reduction mechanisms. A durability study was conducted with the best performing OER catalyst, the 50 wt% NiO/CNT material, in which 1000 anodic sweeps were performed and the catalysts' onset potential and current density were recorded as shown in Fig. 4. In cases of amorphous carbon present in the material, there will be visible and electrochemical degradation, which poisons the electrolyte and leads to a drop in activity. Cyclic voltammetry can be used for determining the durability of materials based on similar tests

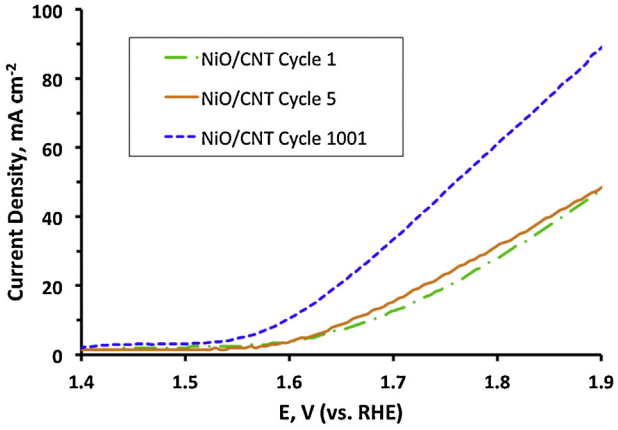

Fig. 4. Electrochemical durability OER data for 50 wt% NiO/CNT catalyst.

that have been performed in the past [23,24]. In the present work, the 50 wt% NiO/CNT catalyst was tested under conditions in which the voltage was increased and decreased between 1.4 and 1.9 V at 10 mV s^{-1}. The term "cycle" refers to the anodic sweep number, where one cycle indicates the current density measurements "up" from 1.4 to 1.9 and "down" from 1.9 back to 1.4 V. The data in Fig. 4 is the sweep "up" from 1.4 to 1.9 V. The catalyst electrochemically improved after 1000 cycles, revealing minimal catalytic deterioration. Visually, the electrolyte was still clear after the durability test, representative of minimal residual amorphous carbon in the catalyst. These results indicate minimal carbon corrosion effects and confirm catalytic stability during bifunctional electrochemical experiments. Anodically, in terms of onset potential, this 50 wt% NiO/CNT catalyst outperforms bulk Ir and bulk Pt in anodic sweeps based on the results reported by Reier et al. [23].

From this series of 50 wt% MO_x/CNT catalysts, based on RDE results, the most active catalyst for ORR is the 50 wt% MnO_2/CNT catalyst and the most active for OER is the 50 wt% NiO/CNT catalyst. The inherent chemical properties of the catalyst provide promising electrochemical results, rivalling the catalytic capabilities of PGM-based materials [20–23]. Furthermore, by understanding the morphology of what makes catalysts different and comparing this to their electrochemical data, one can gain insight as to the particle size, shape and distribution that dictates an active catalyst from one that is deficient.

4. Conclusion

A novel synthesis method was developed in which high purity, functionalized CNTs which allow for the deposition of metal oxide nanoparticles onto the graphitic surfaces, forming bi-functional catalysts. This state-of-the-art synthesis has resulted in catalysts significantly better than other non-PGM published results. The catalytic activity of the 50 wt% MnO_2/CNT catalyst is comparable to carbon-supported Pt-based catalysts for ORR [21,22] and the 50 wt% NiO/CNT onset potential is within 50 mV for Ru and Ir-based catalysts for OER [23] and comparable with manganese-based perovskites reported by Benhangi et al. [25]. This was the first usage of SSM for the synthesis of functionalized CNTs with controlled morphology. By altering the sacrificial supports and crystallite seeds, it is possible to control the thickness of the CNTs, the resulting surface areas and the electrochemical performance of the final materials. There was successful deposition of high loadings of transition metal oxides onto the walls of the CNTs. This article uncovers morphological insight into the characteristic qualities that determine highly active catalyst properties. A series of

systematic experiments, in which the NiO and MnO_2 loadings onto the CNTs are optimized to yield the best bi-functional catalyst from the materials used in this study, is ongoing.

The electrochemical characteristics from the RDE experimentation reveal that the catalysts are bi-functionally active and can act as a replacement for conventional PGM catalysts in the appropriate conditions.

Acknowledgements

The authors are thankful to Aaron Roy for XRD analyses and Dr. Kateryna Artyushkova for XPS analyses.

References

[1] E. Antolini, Appl. Catal. B: Environ. 88 (2009) 1–24.
[2] S. Pylypenko, S. Mukherjee, T.S. Olson, P. Atanassov, Electrochim. Acta 53 (2008) 7875–7883.
[3] M.H. Robson, A. Serov, K. Artyushkova, P. Atanassov, Electrochim. Acta 90 (2013) 656–665.
[4] S. Brocato, A. Serov, P. Atanassov, Electrochim. Acta 87 (2013) 361–365.
[5] A. Serov, M.H. Robson, K. Artyushkova, P. Atanassov, Appl. Catal., B: Environ. 127 (2012) 300–306.
[6] A. Serov, M.H. Robson, M. Smolnik, P. Atanassov, Electrochim. Acta 80 (2012) 213–218.
[7] A. Serov, U. Martinez, A. Falase, P. Atanassov, Electrochem. Commun. 22 (2012) 193–196.
[8] A. Serov, M.H. Robson, B. Halevi, K. Artyushkova, P. Atanassov, Electrochem. Commun. 22 (2012) 53–56.
[9] A. Falase, M. Main, K. Garcia, A. Serov, C. Lau, P. Atanassov, Electrochim. Acta 66 (2012) 295–301.
[10] A. Serov, U. Martinez, P. Atanassov, Electrochem. Commun. 34 (2013) 185–188.
[11] A. Serov, M.H. Robson, M. Smolnik, P. Atanassov, Electrochim. Acta 109 (2013) 433–439.
[12] A. Serov, K. Artyushkova, P. Atanassov, Adv. Energy Mater. 4 (2014) 1301735.
[13] A. Zalineeva, A. Serov, M. Padilla, U. Martinez, K. Artyushkova, S. Baranton, C. Coutanceau, P. Atanassov, J. Am. Chem. Soc. 136 (2014) 3937–3945.
[14] A. Serov, A. Aziznia, P.H. Benhangi, K. Artyushkova, P. Atanassov, E. Gyenge, J. Mater. Chem. A 1 (2013) 14384–14391.
[15] J. Li, N. Wang, Y. Zhao, Y. Ding, L. Guan, Electrochem. Commun. 13 (2011) 698–700.
[16] Z. Chen, A. Yu, R. Ahmed, H. Wang, H. Li, Z. Chen, Electrochim. Acta 69 (2012) 295–300.
[17] K. Mette, A. Bergmann, J.P. Tessonnier, M. Hävecker, L. Yao, T. Ressler, R. Schlogl, P. Strasser, M. Behrens, ChemCatChem 4 (2012) 851–862.
[18] Y. Liang, H. Wang, P. Diao, W. Chang, G. Hong, Y. Li, M. Gong, L. Xie, J. Zhou, J. Wang, T.Z. Regier, F. Wie, H. Dai, J. Am. Chem. Soc. 134 (2012) 15849–15857.
[19] J. Suntivich, H.A. Gasteiger, N. Yabuuchi, H. Nakanishi, J.B. Goodenough, Y. Shao-Horn, Nat. Chem. 3 (2011) 546–550.
[20] W.C. Fang, O. Chyan, C.L. Sun, C.T. Wu, C.P. Chen, K.H. Chen, L.C. Chen, J.H. Huang, Electrochem. Commun. 9 (2007) 239–244.
[21] H.A. Gasteiger, S.S. Kocha, B. Sompalli, F.T. Wagner, Appl. Catal. B: Environ. 56 (2005) 9–35.
[22] J. Greeley, I.E.L. Stephens, A.S. Bondarenko, T.P. Johansson, H.A. Hansen, T.F. Jaramillo, J. Rossmeisl, I. Chorkendorff, J.K. Nørskov, Nat. Chem. 1 (2009) 552–556.
[23] T. Reier, M. Oezaslan, P. Strasser, ACS Catal. 2 (2012) 1765–1772.
[24] S.C. Ball, et al., J. Power Sources 171 (2007) 18–25.
[25] P.H. Benhangi, A. Alfantazi, E. Gyenge, Electrochim. Acta 123 (2014) 42–50.